Pick, U., & Bassilian, S. (1981) *FEBS Lett. 123*, 127–130.
Pick, U., & Karlish, S. J. D. (1980) *Biochim. Biophys. Acta 626*, 255–261.
Pick, U., & Karlish, S. J. D. (1982) *J. Biol. Chem. 257*, 6120–6126.
Pickart, C. M., & Jencks, W. P. (1982) *J. Biol. Chem. 257*, 5319–5322.
Pickart, C. M., & Jencks, W. P. (1984) *J. Biol. Chem. 259*, 1629–1643.
Scales, D., & Inesi, D. (1976) *Biophys. J. 16*, 735–751.
Schwarzenbach, G., Senn, H., & Anderegg, G. (1957) *Helv. Chim. Acta 40*, 1886–1900.
Silva, J. L., & Verjovski-Almeida, S. (1983) *Biochemistry 22*, 707–716.
Stahl, N., & Jencks, W. P. (1987) *Biochemistry 26*, 7654–7667.
Takisawa, H., & Tonomura, Y. (1979) *J. Biochem. (Tokyo) 86*, 425–441.
Van Etten, R. L., Waymack, P. P., & Rehkop, D. M. (1974) *J. Am. Chem. Soc. 96*, 6782–6785.

Characterization of the Ethenoadenosine Diphosphate Binding Site of Myosin Subfragment 1. Energetics of the Equilibrium between Two States of Nucleotide·S1 and Vanadate-Induced Global Conformation Changes Detected by Energy Transfer†

Raul Aguirre,‡,§ Shwu-Hwa Lin,∥ Frances Gonsoulin,§ Chien-Kao Wang,§ and Herbert C. Cheung*,§
Department of Biochemistry and Graduate Program in Biophysical Sciences, University of Alabama at Birmingham, Birmingham, Alabama 35294

Received February 8, 1988; Revised Manuscript Received August 18, 1988

ABSTRACT: The fluorescence decay of 1,N^6-ethenoadenosine diphosphate (ϵADP) bound to myosin subfragment 1 (S1) was studied as a function of temperature. The decay was biexponential, and the two lifetimes were quenched relative to the single lifetime of free ϵADP. The temperature dependence of the fractional intensities of the decay components showed two states of the S1·ϵADP complex. At pH 7.5 in 30 mM TES, 60 mM KCl, and 3 mM $MgCl_2$, the equilibrium constant for the conversion of the low-temperature state ($S1_L$·ϵADP) to the high-temperature state ($S1_H$·ϵADP) was 40 at physiological temperatures, and $\Delta H°$ = 13 kcal·mol^{-1} and $\Delta S°$ = 49 cal·deg^{-1}·mol^{-1}. At 10 °C the equilibrium constant of S1 for ϵADP was 5, indicating that $S1_H$·ϵADP was the dominant state, and that for the vanadate complex ϵADP·Vi was 0.7, suggesting that in S1·ϵADP·Vi the dominant state of the S1–nucleotide complex was converted from $S1_H$·ϵADP to $S1_L$·ϵADP. The single rotational correlation time of bound ϵADP at 10 °C decreased from 107 ns in S1·ϵADP to 74 ns in $S1^+$·ϵADP·Vi. Conversion of the binary complex to the ternary vanadate complex resulted in a 3-Å decrease in the energy transfer distance between bound ϵADP and *N*-[4-(dimethylamino)-3,5-dinitrophenyl]maleimide attached to SH_1 and a decrease of the average distance between bound ϵADP and bound Co^{2+} from 12.6 to 8.3 Å. On the assumption that $S1^+$·ADP·Vi is a good stable analogue of S1·ADP·P_i, it is suggested that the transition $S1_L$·ϵADP → $S1_H$·ϵADP is involved in the power stroke of the contractile cycle. The structural changes that S1 experiences during this transition may include a small increase in dimensional asymmetry and movements of two regions of the heavy chain toward the adenine-binding site.

Elucidation of the mechanism of the cyclic interactions of myosin with ATP and actin requires detailed knowledge of the conformation of myosin subfragment 1 at which the nucleotide- and actin-binding sites are located. The knowledge must include the gross conformation of S1[1] and the conformations of the ATPase site and the actin-binding sites. Several fluorescent nucleotide analogues are available for investigation of nucleotide binding to a variety of proteins. The 1,N^6-ethenoadenosine derivatives are particularly well suited for this purpose because of a high degree of structural similarity to the parent adenine-containing compounds and favorable spectral properties that minimize background interference arising from aromatic amino acid residues. We (Garland & Cheung, 1976, 1979) previously investigated the kinetics and mechanism of the binding of ϵADP and ϵATP to S1 and heavy meromyosin and showed that the binding constants of S1 for ϵADP obtained from equilibrium dialysis and kinetic experiments were in good agreement with each other and with those obtained for ADP by other investigators. The early association constants of S1 for ϵADP were recently confirmed in an equilibrium polarization study by Perkins et al. (1984a).

The orthovanadate ion is an inhibitor of myosin ATPase. Together with ADP, Vi binds stoichiometrically to the active site of the enzyme and forms an inactive complex (Goodno, 1982). On the basis of the kinetics of ATPase inhibition, it

† This work was supported by NIH Grant AR31239.
* Author to whom correspondence should be addressed.
‡ Present address: Department of Biochemistry, University of Chile, Santiago, Chile.
§ Department of Biochemistry.
∥ Graduate Program in Biophysical Sciences.

[1] Abbreviations: S1, myosin subfragment 1; ϵADP, 1,N^6-ethenoadenosine diphosphate; ϵATP, 1,N^6-ethenoadenosine 5′-triphosphate; Vi, orthovanadate ion; DDPM, *N*-[4-(dimethylamino)-3,5-dinitrophenyl]-maleimide; TES, *N*-[tris(hydroxymethyl)methyl]-2-aminoethanesulfonic acid; DTT, dithiothreitol; NEM, *N*-ethylmaleimide; FRET, fluorescence resonance energy transfer; IAEDANS, *N*-(iodoacetyl)-*N*′-(5-sulfo-1-naphthyl)ethylenediamine.

0006-2960/89/0428-0799$01.50/0

has been proposed that the initial ternary complex M·ADP·Vi undergoes a slow transition to a stable complex, denoted M^+·ADP·Vi. This stable complex is believed to be an analogue of the steady-state intermediate M^{**}·ADP·P_i of the Mg^{2+}-dependent ATPase pathway. X-ray diffraction studies with glycerinated muscle have suggested a conformational analogy between M^{**}·ADP·P_i and M^+·ADP·Vi (Goody et al., 1980). A spin-label attached to the reactive thiol SH_1 of myosin was exploited to demonstrate that the complex M^+·ADP·Vi was a good analogue of M^{**}·ADP·P_i (Wells & Bragshaw, 1984). Ample evidence (Morita, 1967; Cheung, 1970; Seidel & Gergely, 1971; Werber et al., 1972) exists demonstrating a conformational difference between M^{**}·ADP·P_i and the binary complex M^*·ADP that is formed at the end of the ATP hydrolysis reaction. Formation of a stable analogue of M^{**}·ADP·P_i with Vi allows convenient investigation of the properties of the intermediate species. The use of Vi to trap nucleotide has an advantage over cross-linking the two reactive thiols SH_1 and SH_2 (Cys 707 and Cys 697, respectivley, in S1) (Wells & Yount, 1982) because free thiols are available for modification with spectroscopic probes. By using the fluorescent probes 5-(iodoacetamido)fluorescein and (iodoacetamido)salicylate attached to SH_1, we (Aguirre et al., 1986) observed a slow transition of the initial ternary complex S1·ADP·Vi formed between labeled S1, ADP, and Vi to a stable, long-lived complex, $S1^+$·ADP·Vi, with a rate constant of (5–7) × 10^{-3} s^{-1}. S1·ADP·Vi had a fluorescence state identical with that of S1·ADP obtained with labeled S1 and a more open structure in the SH_1 region than uncomplexed labeled S1. Transition of S1·ADP·Vi to $S1^+$·ADP·Vi resulted in a more open structure of the SH_1 region than in S1·ADP·Vi.

In the present study we investigated the emission properties of εADP bound to S1 over the temperature range 2–26 °C. The results demonstrate the existence of two states of S1·εADP. The bound nucleotide was used as a donor of fluorescence resonance energy transfer to estimate its separation from DDPM attached to SH_1 and from bound Co^{2+}, both in the presence and absence of vanadate.

Materials and Methods

Reagents and Chemicals. DDPM, εADP, ADP, ATP, and NEM were obtained from Sigma Chemical Co. (St. Louis, MO). These reagents were used without further purification. Chymotrypsin was obtained from Worthington Diagnostic Systems (Freehold, NJ). $CoCl_2$ was obtained from Spex Industries (Metuchen, NJ) as a standard solution. V_2O_5 (Aldrich Chemical Co., Milwaukee, WI) was used to prepare a stock solution of sodium vanadate as described by Goodno (1982).

Protein Preparations. Myosin was prepared from rabbit skeletal muscle as previously described (Aguirre et al., 1986) by the method of Flamig and Cusanovich (1981). Freshly prepared myosin was used to prepare S1 by chymotryptic digestion as described by Weeds and Taylor (1975). The two isozymes S1(A1) and S1(A2) isolated on a DE-52 column were pooled, dialyzed against ammonium acetate and 0.1 mM DTT, and lyophilized in the presence of 0.1 M sucrose. Actin was prepared from an acetone powder according to the method of Spudich and Watts (1971). A molecular weight of 115000 was used to estimate the concentration of S1 from an absorbance of 0.75 g^{-1}·cm^{-1} at 280 nm. Actin was assumed to have a monomeric molecular weight of 42000 and an absorbance of 0.63 g^{-1}·cm^{-1} at 290 nm.

The sulfhydryl group (SH_1) of Cys 707 of S1 was modified by the nonfluorescent reagent DDPM at 4 °C by incubation of the protein with a 1.2-fold excess of the probe (10 mM) dissolved in acetone for 2 h in a medium containing 60 mM KCl and 30 mM TES at pH 7.5 (buffer A). Occasionally, it was necessary to first dialyze S1 against buffer A plus 0.2 mM DTT, followed by a second dialysis in which DTT was omitted immediately prior to sulfhydryl labeling. Unreacted DDPM was removed by exhaustive dialysis against buffer A. The concentration of DDPM-S1 was determined by the Lowry method using nonlabeled S1 as a standard. The concentration of nonlabeled S1 was independently determined by absorbance at 280 nm. The degree of SH_1 labeling by DDPM was estimated by using a molar extinction coefficient of 2930 cm^{-1} at 442 nm for the probe (Gold & Segal, 1964) and found to be in the range 0.95–0.97. The kinetics and extent of labeling were followed by measurements of Ca^{2+}-activated ATPase activities (Cheung et al., 1983). Labeling of SH_1 by *N*-ethylmaleimide was similarly carried out. The CaATPase activity of both DDPM- and NEM-labeled S1 was enhanced to a similar extent.

Fluorescence Measurements. Steady-state fluorescence measurements were carried out on either a Perkin-Elmer 650/40 ratio spectrofluorometer or a Perkin-Elmer MPF-66 fluorescence module interfaced to a PE 7300 computer. Quantum yields were determined by using the comparative method (Parker & Reese, 1960) with quinine sulfate in 0.05 N H_2SO_4 (quantum yield 0.70) as the standard (Scott et al., 1970). For these measurements the exciting light was polarized at 54° from the horizontal, and the emitted light was measured without polarizer.

Fluorescence lifetimes were measured in a thermostated photon-counting PRA 2000 pulsed nanosecond fluorescence spectrometer as previously described (Aguirre et al., 1986). A Ditric three-cavity 335-nm interference filter was used for excitation of εADP with light polarized at 54° from the horizontal, and a three-cavity 410-nm interference filter was used to isolate its unpolarized emission. The lifetime data were analyzed as previously described (Aguirre et al., 1986). Fluorescence anisotropy decay was determined by using vertically polarized excitation and measuring the fluorescence polarized in the vertical and horizontal directions to obtain the respective intensities $F_\parallel(t)$ and $F_\perp(t)$. This was accomplished by changing the emission polarizer from the vertical to the horizontal position every 20 min until at least 20000 counts were collectd in the peak channel for $F_\parallel(t)$. The $F_\perp(t)$ was accumulated for the same period of time as for $F_\parallel(t)$. For these measurements a Corning 3-74 cutoff filter (cutoff wavelength 370 nm) was used to isolate the emission. The anisotropy decay function was obtained from $F_\parallel(t)$ and $F_\perp(t)$

$$A(t) = \frac{F_\parallel(t) - F_\perp(t)}{F_\parallel(t) + 2F_\perp(t)} \quad (1)$$

and deconvoluted by a nonlinear least-squares algorithm (Grinvald & Steinberg, 1974). The $A(t)$ function was assumed to follow an exponential or a sum of exponential decay law:

$$A(t) = \sum_{i=1}^{3} c_i \exp(-t/\phi_i) \quad (2)$$

The characteristic decay times (rotational correlation times) ϕ_i depend on the rotational diffusion coefficients, which in turn depend upon the size and axial ratio of the macromolecule. The preexponential coefficients c_i are functions of the orientations of the absorption and emission dipoles in the protein. For monoexponential decay $A(t) = A_0 \exp(-t/\phi)$, where $A_0 = A(0)$ is the limiting anisotropy observed at zero time. The statistical criteria used to judge the goodness of fits between observed data and the calculated values were (1) the Dur-

Table I: Temperature Dependence of Fluorescence Decay of ϵADP in the S1·ϵADP Complex[a]

temp (°C)	τ_1 (ns)	α_1	τ_2 (ns)	α_2
4.4	23.9	0.65	10.4	0.35
11.0	23.6	0.67	9.6	0.33
13.3	23.4	0.68	9.2	0.32
15.6	24.3	0.72	9.0	0.28
16.4	24.5	0.73	8.9	0.27
18.7	23.9	0.70	6.8	0.30
20.0	23.0	0.75	7.2	0.25
20.7	24.2	0.73	7.6	0.27
21.7	24.7	0.78	7.5	0.22
22.9	24.7	0.79	6.4	0.21
24.4	24.5	0.79	5.6	0.21
25.6	24.6	0.79	5.4	0.21

[a] Conditions: 10 μM ϵADP, 20 μM S1, 2 mM $MgCl_2$, 60 mM KCl, and 30 mM TES, pH 7.5. The parameters for each temperature were averages from three to six different measurements with three different protein preparations. The uncertainty (standard error) was 2% or less for τ_1 and less than 5% for τ_2 between 4 and 22 °C, and about 10% above 22 °C. The uncertainty in amplitudes was less than 3% for α_1 and less than 10% for α_2.

bin–Watson number, (2) the reduced χ^2 value, (3) the autocorrelation function of the weighted residuals, and (4) the weighted residuals.

The efficiency of FRET was determined by measuring either steady-state donor intensity or donor lifetime (Wang & Cheung, 1986):

$$E = 1 - \frac{F_{da} - F_d(1 - f_a)}{F_d f_a} \quad (3)$$

$$E = 1 - \tau_{da}/\tau_d \quad (4)$$

where F_{da} is the donor fluorescence intensity determined in the presence of the acceptor, F_d is the donor intensity in the absence of the acceptor, f_a is the fractional occupancy of acceptor site in the sample containing both donor and acceptor, τ_{da} is the donor lifetime in the presence of acceptor, and τ_d is the donor lifetime in its absence. The measured transfer efficiency E is related to the donor–acceptor separation R and the Förster critical distance R_0 by

$$E = R_0^6/(R_0^6 + R^6) \quad (5)$$

R_0 is given by

$$R_0^6 = (8.79 \times 10^{-5}) n^{-4} Q J \kappa^2 \quad (\text{Å}^6) \quad (6)$$

where n is the refractive index of the medium between donor and acceptor (taken as 1.4), Q is the donor quantum yield measured in the absence of acceptor, J is the spectral overlap integral between donor emission and acceptor absorption expressed in units of $M^{-1}\cdot cm^{-1}\cdot nm^4$, and κ_2 is the orientation factor of the donor emission and acceptor absorption dipoles. J is given by

$$J = \int_0^\infty F_d(\lambda)\epsilon_a(\lambda)\lambda^4\, d\lambda \Big/ \int_0^\infty F_d(\lambda)\, d\lambda \quad (7)$$

where $F_d(\lambda)$ is the corrected emission spectrum of the donor expressed in an arbitrary unit and $\epsilon_a(\lambda)$ is the extinction coefficient of bound acceptor expressed in units of $M^{-1}\cdot cm^{-1}$. J was numerically integrated at 1-nm intervals.

Results

Fluorescence Decay of ϵADP Bound to S1. The emission of ϵADP bound to S1 was measured as a function of temperature. None of the decay curves could be fitted to a single exponential, but they all could be fitted to a biexponential model yielding two lifetimes. A typical decay curve is shown in Figure 1. Listed in Table I are the best fitted decay parameters for the temperature range 4–26 °C. The long lifetime (τ_1) was relatively insensitive to variation in temperature, but the short component generally decreased with increasing temperature over the narrow range studied. The fractional amplitudes shifted in favor of the component (α_1) associated with the long lifetime. The two-exponential characteristic of the decay persisted down to the lowest temperature (2 °C) studied at which α_1 was still larger than 0.5 (data not shown). Since the decay of free ϵADP at pH 7.5 and 4 °C is single exponential with $\tau = 27.4 \pm 0.2$ ns (Harvey & Cheung, 1977), the question arose as to whether the observed τ_1 could have originated from free ϵADP. We attempted to fit several sets of the low-temperature data to a biexponential function by fixing τ_1 at 27 ± 1 ns and to a triexponential function without constraint on any of the lifetimes. No satisfactory fits could be obtained in these trials. We also measured the decay with samples in which the ratio [ϵADP]/[S1] was varied in the range 0.5–0.1 at 4 and 10 °C. In every case α_1 was substantially above 0.5. Since under some of these conditions there was essentially no free ϵADP (Garland & Cheung, 1976), the biexponential decay must be a characteristic of S1·ϵADP.

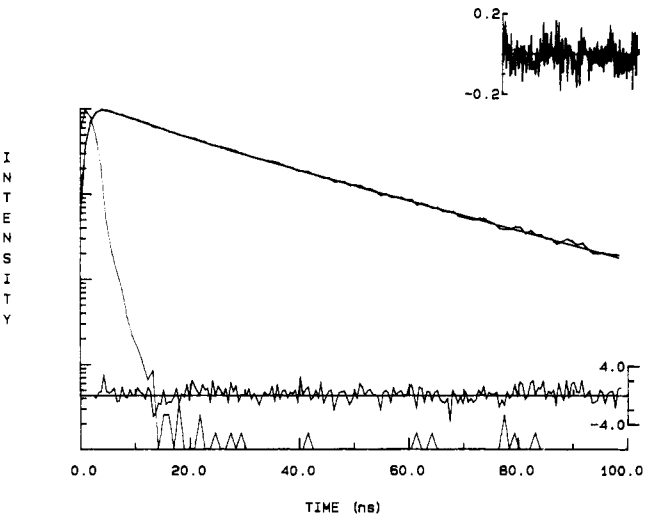

FIGURE 1: Fluorescence decay of ϵADP in the complex S1·ϵADP. The sample contained 10 μM ϵADP, 20 μM S1, 60 mM KCl, 30 mM TES, and 2 mM $MgCl_2$, pH 7.5, at 16 °C. The sharp peak on the left is the lamp profile. The solid curve is the best fit of the data to a biexponential function yielding two lifetimes: $\tau_1 = 24.91$ ns and $\tau_2 = 9.83$ ns with corresponding fractional amplitudes $\alpha_1 = 0.72$ and $\alpha_2 = 0.28$. The upper panel shows the autocorrelation function of the weighted residuals between observed data and the chosen function. The lower tracing across the plot shows the deviation between the calculated and experimental values, corresponding to a reduced χ^2 value (χ^2_R) of 1.04 and a Durbin–Watson (D-W) parameter of 1.80. A D-W value of 1.75 indicates perfect fitting of the data to a biexponential function.

The two fractional intensities (f_1 and f_2) associated with the two decay components are given by $f_1 = \alpha_1\tau_1/(\alpha_1\tau_1 + \alpha_2\tau_2)$ and $f_2 = \alpha_2\tau_2/(\alpha_1\tau_1 + \alpha_2\tau_2)$. They provide a measure of the relative intensities of the two components. A plot of f_1/f_2 vs temperature depicted in Figure 2 shows a transition in the range 15–25 °C. The shape of the curve suggests a two-state equilibrium. If the two lifetimes reflect the presence of two states of S1·ϵADP and if the two states are in equilibrium under our experimental conditions, the ratio f_1/f_2 is an equilibrium constant (K_{eq}) for the transition of state 2 (associated with the short τ_2) to state 1: $(\text{state})_2 \rightleftarrows (\text{state})_1$. State 2 ($S1_L\cdot\epsilon ADP$) was favored at low temperature, and state 1

Table II: Anisotropy Decay Parameters for εADP Bound to S1[a]

			lifetimes							
			recovered from polarized decay				from magic-angle excitation			
complex	ϕ (ns)	$A(0)$	τ_1 (ns)	α_1	τ_2 (ns)	α_2	τ_1 (ns)	α_1	τ_2 (ns)	α_2
S1·εADP	107 ± 3	0.226	21.1	0.67	9.3	0.33	21.0	0.70	9.3	0.30
S1·εADP·Vi	74 ± 3	0.219	22.7	0.37	11.2	0.63	20.9	0.26	11.4	0.74

[a] Conditions: 10 °C, 60 mM KCl, 2 mM $MgCl_2$, 30 mM TES, pH 7.5, 201 μM S1, 38–64 μM εADP, and 0.4 mM Vi (when present).

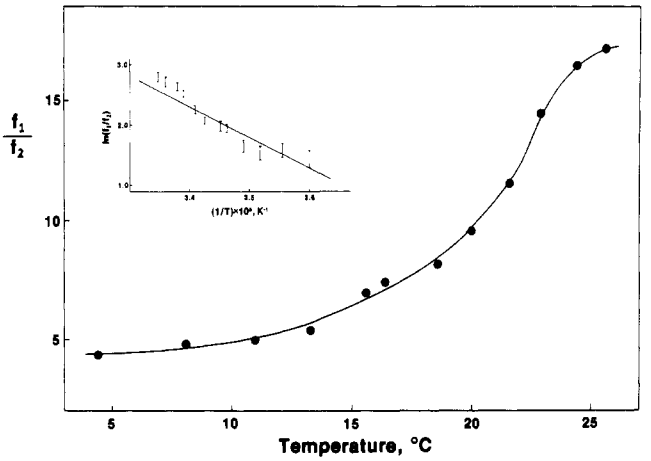

FIGURE 2: Temperature dependence of the ratio of fractional intensities (f_1/f_2) of εADP in the complex S1·εADP. Conditions were the same as those listed in Table I. The inset shows log (f_1/f_2) as a function of reciprocal temperature (coefficient of correlation 0.97). The change in enthalpy was obtained from the slope of the line.

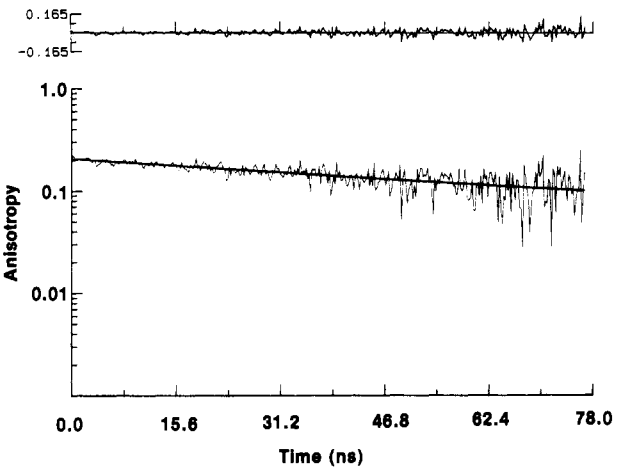

FIGURE 3: Fluorescence anisotropy decay of εADP in S1·εADP. The sample contained 17 μM εADP, 100 μM S1, 60 mM KCl, 30 mM TES, and 2 mM $MgCl_2$, pH 7.5 at 10 °C. The decay was fitted to a single-exponential model yielding a single rotational correlation time ϕ = 110 ± 3 ns. The anisotropy at zero time $A(0)$ was 0.229. This was a three-parameter fit (one rotational correlation time and two lifetimes), which was characterized by a reduced χ^2 value (χ^2_R) of 1.01 and a D-W parameter of 2.09. A D-W parameter of 2.0 corresponds to a perfect three-parameter fit for the data.

($S1_H$·εADP) predominated at high temperature. The data given in Table II were analyzed by the van't Hoff equation, yielding $\Delta H°$ = 13 ± 1 kcal·mol^{-1} (54.3 kJ) and $\Delta S°$ = 49 ± 4 cal·deg^{-1}·mol^{-1} (205 J).

Anisotropy Decay of Bound εADP and Effect of Vanadate on εADP Emission. The anisotropy decay of εADP bound to S1 was determined in two conditions: (1) 64 μM εADP + 201 μM S1 and (2) 38 μM εADP + 201 μM S1. Essentially identical results were obtained from both sets of measurements. A typical anisotropy decay curve is shown in Figure 3, and the decay parameters are given in Table II. All decay curves were very well fitted to a single exponential function. The rotational correlation time was 107 ns, and the limiting anisotropy $A(0)$ was 0.226. Since the fundamental anisotropy of ε-adenosine and εATP is at least 0.32 when excited in the range 330–350 nm (Cheung & Liu, 1984), εADP bound to the nucleotide site of S1 had considerable motional freedom.

In the presence of vanadate, both the fluorescence decay and anisotropy decay were altered (Table II). While the fluorescence decay remained biexponential and the two lifetimes were relatively unchanged, the fractional amplitudes were significantly affected. The ratio α_1/α_2 was reduced from 2.32 to 0.36, and f_1/f_2 was redcued to 0.66. The net effect was a decrease in the average lifetime from 17.4 to 13.9 ns. The same changes were observed regardless of whether the lifetimes were (1) determined by measuring unpolarized decay with magic angle excitation or (2) recovered from the two perpendicular components of polarized decay in conjunction with determination of anisotropy decay by using the equation $F(t) = F_{\parallel}(t) + 2F_{\perp}(t)$. These changes were in the same direction as those observed with decreasing temperature in the absence of Vi. In terms of a two-state equilibrium for S1·εADP, over the temperature range studied the high-temperature state was the dominant species, and the proportion of the low-temperature state (α_2) was substantially less than 0.5. Vi binding to the binary complex drove the equilibrium far toward the low-temperature state, and at 10 °C the low-temperature state became the dominant species. This transition was accompanied by a 30% decrease of the rotational correlation time, while the limiting anisotropy was little effected.

Energy Transfer between Bound εADP and SH_1. The emission spectrum of bound εADP has a maximum at 408.5 nm. It overlaps the absorption spectrum DDPM covalently attached to SH_1. FRET measurements were carried out for the separation between bound εADP and DDPM attached to SH_1. The quantum yield of donor εADP bound to S1 and the steady-state intensity of bound donor (F_d) were determined with S1 that had been modified at SH_1 by NEM. The use of NEM-labeled S1 for these measurements allowed separation of the effect of acceptor labeling from the effect of resonance energy transfer on the donor emission properties. The effect of Vi and the effect of formation of rigor acto-S1·εADP on the nucleotide site-SH_1 distance were determined. These results are summarized in Table III. The axial depolarization factor of bound εADP was determined from the measured limiting anisotropy and the previously determined fundamental anisotropy of the ethenoadenine group. There is some ambiguity on the value of the axial depolarization factor because the anisotropy of the bound εADP decreases across the emission band (Perkins et al., 1984a). The origin of this variation is obscured, but phenomenologically the limiting anisotropy determined with a cutoff filter is still a useful parameter to indicate the average extent of depolarization. This procedure was used to obtain $A(0)$. Although it is not possible to determine the mobility of the acceptor DDPM because it was nonfluorescent, it was still possible to estimate the upper and lower bounds for the orientation factor (κ^2) and to estimate the maximum and minimum values of the do-

Table III: FRET Distances between Bound ϵADP and DDPM Attached to SH_1 of S1[a]

	S1(DDPM)·ϵADP	S1(DDPM)·ϵADP·Vi	acto·S1-(DDPM)·ϵADP
E	0.38	0.44	0.45
Q	0.45	0.35	0.50
J ($M^{-1}\cdot cm^{-1}\cdot nm^4$)	8.82×10^{13}	8.20×10^{13}	9.79×10^{13}
$R_0(2/3)$ (Å)	29.2	27.5	31.1
R(max) (Å)	37.5	38.7	36.9
$R(2/3)$ (Å)	31.6	28.7	30.1
R(min) (Å)	20.5	20.1	20.2

[a] Conditions: 60 mM KCl, 2 mM $MgCl_2$, 30 mM TES, pH 7.5, 10 μM S1, 5 μM ϵADP, and 20 °C. E was calculated from donor steady-state intensity (eq 1). S1(DDPM) is S1 labeled at SH_1 with DDPM. The degree of acceptor (DDPM) labeling was 0.97. Quantum yields (Q) used to calculate the overlap integral (J) for S1-(DDPM)·ϵADP·Vi and for acto·S1(DDPM)·ϵADP were determined in the presence of Vi and actin, respectively (see text for other details). The axial depolarization factor for ϵADP in S1·ϵADP was calculated from $(A_0/A_f)^{1/2}$ and was 0.886, where A_0 was the measured limiting anisotropy [$A(0)$] of bound ϵADP determined from anisotropy decay and A_f was the fundamental anisotropy of ϵADP (see text). In the presence of Vi this depolarization factor for ϵADP was 0.806. The value 0.886 was taken as the depolarization factor for ϵADP in acto·S1(DDPM)·ϵADP. From these factors the maximum and minimum values of the orientation factor [κ_2(max) and κ_2(min)] were calculated (Dale et al., 1979; Wang & Cheung, 1986). R(max) and R(min) are the corresponding maximum and minimum values of the donor–acceptor separation. $R(2/3)$ is the distance calculated on the basis of $\kappa^2 = 2/3$ (rapid and isotropic orientations of probe dipoles).

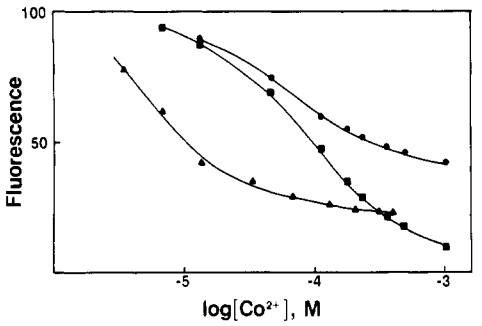

FIGURE 4: Fluorescence intensity of ϵADP bound to S1 as a function of the concentration of added $CoCl_2$ in 60 mM KCl and 30 mM TES, pH 7.5 at 20 °C: (■) 8 μM ϵADP + 20 μM S1; (●) 8 μM ϵADP + 20 μM S1 + 100 μM $MgCl_2$; (▲) 8 μM ϵADP + 20 μM S1 + 100 μM Vi incubated 90 min after addition of $CoCl_2$. Excitation at 335 nm and emission isolated at 410 nm.

nor–acceptor separation, R(max) and R(min). The use of the value $R(2/3)$ based on $\kappa^2 = 2/3$ (rapid and isotropic motions of donor and acceptor dipoles) to represent the donor–acceptor distance was not justified in this case. The error in using $R(2/3)$ to describe the ϵADP–SH_1 distance could be considerable when compared to R(max) and R(min). This uncertainty aside, the distance may be shorter in the stable ternary $S1^+$·ϵADP·Vi complex than in the binary complex. The difference, however, is marginal. There was no evidence for an altered distance in S1 when the protein was incorporated into the rigor acto·S1·ϵADP complex.

Effect of Co^{2+} on Emission Properties of S1·ϵADP. The steady-state fluorescence intensity of ϵADP in S1·ϵADP was quenched by the addition of Co^{2+} in the concentration range of 10^{-6}–10^{-3} M. The quenching was significantly less effective in the presence of Mg^{2+} (Figure 4), suggesting a competition between Co^{2+} and Mg^{2+} for the same sites in S1. In the presence of Vi (and in the absence of Mg^{2+}) the quenching of Co^{2+} was considerably enhanced with a 50% quenching at about 1×10^{-5} M Co^{2+}. This Co^{2+} concentration was 1 order of magnitude smaller than that required for the same extent

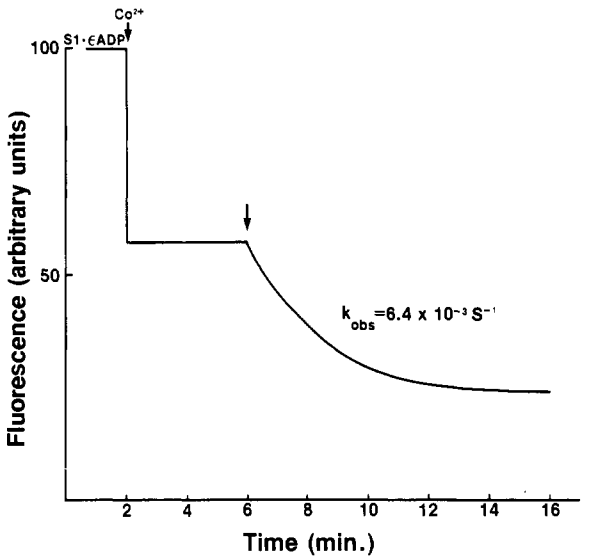

FIGURE 5: Changes of fluorescence intensity of 8 μM ϵADP + 16 μM S1 after sequential addition of 100 μM $CoCl_2$ and 100 μM Vi. Other conditions: 60 mM KCl, 30 mM TES, pH 7.5, and 20 °C. Excitation at 335 nm and emission isolated at 410 nm.

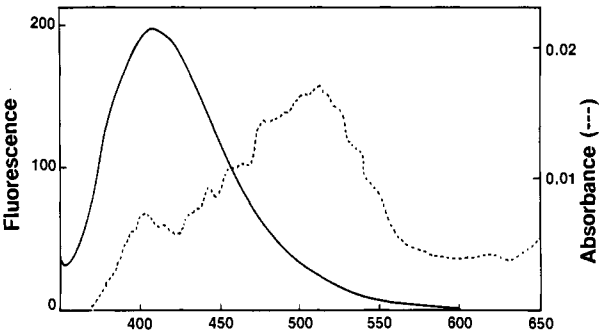

FIGURE 6: Corrected emission spectrum (—) of 5 μM ϵADP + 10 μM S1 with excitation at 335 nm and absorption spectrum (---) of 1 mM $CoCl_2$ in the presence of 1.1 mM bovine serum albumin. Conditions: 60 mM KCl, 30 mM TES, 2 mM $MgCl_2$, pH 7.5, and 20 °C.

of quenching in the absence of Vi. The time course for the effect of sequential addition of Co^{2+} and Vi on the fluorescence of S1·ϵADP is shown in Figure 5. Quenching by Co^{2+} was very rapid, but the additional quenching to a stable fluorescence level by subsequent addition of Vi was slow with a rate constant of 6.4×10^{-3} s^{-1}. Vi alone also quenched S1·ϵADP in the presence of Mg^{2+} with a rate constant of 4.8×10^{-3} s^{-1} (data not shown). This quenching is consistent with the observed reduction of the average lifetime of S1·ϵADP in the presence of Vi.

The rapid quenching of S1·ϵADP by Co^{2+} may be interpreted in terms of the Förster type of fluorescence resonance energy transfer from bound ϵADP to bound Co^{2+}. Although the transfer cannot be unequivocally demonstrated through measurements of sensitized acceptor emission because the acceptor is not fluorescent, Figure 6 provides support of this interpretation. The overlap between the emission and absorption spectra is small but sufficient to cause energy transfer from ϵADP to Co^{2+} both bound to S1. The average lifetime of bound ϵADP in S1·ϵADP was 18.61 ns at 13 °C. In the presence of 0.1 mM $CoCl_2$ the two lifetimes were $\tau_1 = 20.78$ ns ($\alpha_1 = 0.28$) and $\tau_2 = 8.70$ ($\alpha_2 = 0.72$) and $\langle\tau\rangle = 12.08$ ns ($\chi^2_R = 1.38$). From these data the transfer efficiency E was found to be 0.35, corresponding to a donor–acceptor distance $R(2/3)$ of 12.6 Å (Table IV). Essentially the same results were obtained by the steady-state intensity method. In

Table IV: FRET Distances between ϵADP and Co^{2+} Bound to S1[a]

	S1·ϵADP·Co	S1·ϵADP·Co·Vi
E	0.35	0.69
Q	0.47	0.40
J ($M^{-1}\cdot cm^{-1}\cdot nm^4$)	3.07×10^{11}	2.91×10^{11}
$R_0(2/3)$ (Å)	11.4	9.2
R(max) (Å)	14.1	9.2
$R(2/3)$ (Å)	12.6	8.3
R(min) (Å)	11.5	7.6

[a] Conditions: 60 mM KCl, 2 mM $MgCl_2$, 30 mM TES, pH 7.5, 40 μM S1, 20 μM ϵADP, and 13 °C. E was calculated from $E = 1 - \tau_d/\tau_{da}$, where τ_d was the average lifetime ($\langle\tau\rangle$) of bound ϵADP determined with S1·ϵADP or S1·ϵADP·Vi and τ_{da} was the average lifetime determined with S1·ϵADP·Co or S1·ϵADP·Co·Vi.

the presence of Vi, the decay of S1·ϵADP was biexponential with $\langle\tau\rangle = 14.1$ ns. When Co^{2+} was also present, the decay of ϵADP in ϵADP + S1 + Vi + Co^{2+} was biexponential with $\tau_1 = 19.38$ ns ($\alpha_1 = 0.16$), $\tau_2 = 2.14$ ns ($\alpha_2 = 0.84$), and $\langle\tau\rangle = 4.89$ ns ($\chi^2_R = 1.21$). Implicit in our conclusion of energy transfer between ϵADP and Co^{2+} is the assumption that binding of the cation per se does not lead to quenching of the emission of the bound donor. On this basis and the further assumption that vanadate has no effect on the extent of Co^{2+} binding, the additional quenching of the donor emission induced by vanadate may be taken as evidence of enhanced energy transfer. Thus the transfer efficiency from ϵADP to Co^{2+} in the presence of Vi was 0.65, corresponding to $R(2/3) = 8.3$ Å (Table IV). Formation of a stable ternary complex $S1^+$·ϵADP·Vi shortened the separation between bound ϵADP and bound Co^{2+} by over 4 Å. Since Co^{2+} is thought to be an isotropic oscillator with a triply degenerate transition, its axial depolarization can be taken as zero. The value of $R(2/3)$ differs from the upper and lower limits by only 12% or less. In this case it is reasonable to use $R(2/3)$ to represent the donor–acceptor separation.

It is noted that the stoichiometry of bound Co^{2+} was unknown and could be above 1.0 although there was evidence that Co^{2+} may compete with Mg^{2+} for the same site. For the case of energy transfer from a single donor to n acceptors, a simple expression can be derived relating the observed transfer efficiency to an apparent distance. If it is assumed that the n acceptors are symmetrically located with respect to the donor so that the n transfer distances are equivalent, the distance (R') between the donor and any one of the acceptors is given by (Rao, 1979; Highsmith & Murphy, 1984)

$$R' = n^{1/6}R \quad (8)$$

where R is the distance for a single donor–acceptor pair calculated from the observed transfer efficiency and n is the number of acceptors. For $n = 2$, $R' = 1.11R$ and for $n = 3$, $R' = 1.20R$. The R values listed in Table III are the lower limits. In spite of these uncertainties, the results demonstrate a structural difference between the binary and ternary complexes.

Discussion

In a previous study we (Aguirre et al., 1986) showed that the signals from two different fluorophores covalently attached to SH_1 of S1 were sensitive to the presence of ADP and ATP and suggested that S1 existed in two conformations dependent upon occupancy of the nucleotide site. We also suggested that the conformation of S1·ADP in the region of SH_1 was more open than that of S1 in the absence of bound nucleotide. The present study has extended the previous work by using a spectroscopic signal originating from the adenine moiety of bound nucleotide to demonstrate two states of S1·ϵADP. The bound ethenonucleotide has two distinct fluorescence lifetimes in contrast to a single lifetime that was previously reported for free ϵADP. The two states of S1·ϵADP are in equilibrium with each other as reflected by a temperature-induced shift of the fractional intensities associated with the two observed decay components. This shift is clear evidence for the existence of two states of S1·ϵADP. In an extensive study of the kinetic mechanism of the binding of ϵATP and ϵADP to S1 (Garland & Cheung, 1979), it was shown that the kinetic data were compatible with a three-step binding mechanism. This model suggests the presence of two intermediate states of S1–nucleotide that were generated subsequent to the formation of an initial encounter complex. The present results lend support to the previous suggestion based on kinetic data.

Other workers have reported evidence suggesting two states of S1–nucleotide from UV difference spectra (Morita, 1977), oxygen exchange (Sleep & Hutton, 1980), ^{31}P NMR (Shriver & Sykes, 1981a), and kinetic analysis of intrinsic fluorescence signals (Trybus & Taylor, 1982). The present study differs from the others in that the signal reporting the conformation states is localized at the adenine moiety of the nucleotide. There is evidence (Chaussepied et al., 1986) that a single ATP molecule binds to S1 at two different regions of the heavy chain that are far removed from each other in the amino acid sequence, one region for the adenine moiety and the other for the phosphoryl group. The two conformation states reported here differ in the adenine-binding site although the data do not rule out involvement of the other site.

The decay of ϵADP bound to S1 was previously measured by phase fluorometry at a single modulation frequency and found to be single exponential (Perkins et al., 1984a). This decay was first noted to be biexponential from time-domain data obtained at a single temperature (Rosenfeld & Taylor, 1984). Since the Stern–Volmer plot for the S1·ϵADP complex was nonlinear, these investigators attributed the two lifetimes to two states of the complex. We have shown that the short lifetime is associated with the low-temperature state ($S1_L$·ϵADP) and this lifetime increases by 70% with decreasing temperature over a narrow range. This increase suggests a change in either (1) the conformation of the adenine-binding site or (2) the interaction of ϵADP with S1 in this state. There appears to be little or no corresponding change for the high temperature state ($S1_H$·ϵADP). Transition from $S1_H$·ϵADP to $S1_L$·ϵADP is accompanied by structural alterations of the adenine-binding site in at least one state. The lifetimes of ϵADP in both states are quenched relative to that of the free nucleotide in aqueous solution. We have previously shown that several amino acids including Cys, Met, and Trp can quench the emission decay of free ϵATP in water and reduce its lifetime to below 10 ns (Harvey & Cheung, 1976). It is not known whether interaction between bound ϵADP and the side chains of neighboring residues at the active site of S1 is responsible for the reduced lifetimes. If such interactions should play a role, they would be more extensive in the low-temperature state than in the high-temperature state. Upon lowering the temperature these interactions would be considerably more weakened in $S1_L$·ϵADP.

In addition to structural differences between the two states as demonstrated here and suggested by a different accessibility of bound ϵADP in the two states to quenching by acrylamide (Rosenfeld & Taylor, 1984), the two states also differ energetically with large $\Delta H°$ and $\Delta S°$ for their interconversion. In spite of the large enthalpy change, the two states differ in free energy by only 2.4 kcal at 37 °C. These thermodynamic values are in close agreement with those previously reported

($\Delta H°$ = 15 kcal·mol^{-1} and $\Delta S°$ = 55 cal·deg^{-1}·mol^{-1}) for the interconversion of the two states of S1·ADP (M^*_RADP → M^*_TADP) on the basis of NMR data (Shriver & Sykes, 1981b). Thus $S1_H$·ϵADP appears similar to the NMR-detected M^*_TADP and $S1_L$·ϵADP to M^*_RADP.

The rotational correlation time of S1·ϵADP directly determined from anisotropy decay is 107 ns at 10 °C. This value is smaller than those previously determined from the anisotropy decay of IAEDANS-attached SH_1 by a factor of 2 (Mendelson et al., 1972, 1973) and by 30% (Botts et al., 1982). The present value, however, is in agreement with that estimated from steady-state anisotropy measurements of ϵADP trapped at the active site by cross-linking SH_1 and SH_2 (Perkins et al., 1984a) and also close to the value calculated for the β-phosphate of bound ADP (Shriver & Sykes, 1981b). The difference in the correlation times obtained by the two different fluorophores may be related to the difference in the orientation of their transition dipoles with respect to the protein axis. The observed limiting anisotropy of bound ϵADP is lower than the fundamental anisotropy expected of the ethenoadenine moiety and shows that the bound adenine undergoes rapid fluctuations in the orientation of its transition dipole. This motion may also contribute to the smaller correlation time observed with bound nucleotide.

In the ternary complex $S1^+$·ϵADP·Vi the rotational correlation time of the bound ϵADP is reduced by 30% from 107 to 74 ns with virtually no change in $A(0)$. This decrease may be due to either (1) a change in the overall shape of S1 in the ternary complex or (2) a substantial realignment of the transition dipoles of the bound nucleotide. An equivalent spherical protein with a hydration of 0.2–0.4 g of H_2O/g of protein has a rotational correlation time of 60–73 ns at 10 °C. Several lines of evidence including the early values of ϕ (Mendelson et al., 1973) and hydrodynamic results (Yang & Wu, 1977) have indicated S1 to be asymmetric. The present ϕ value observed for the binary complex S1·ϵADP can be similarly interpreted. Since $A(0)$ remains unchanged, the 30% decrease in ϕ resulting from formation of S1·ϵADP·Vi may be attributed to a decrease in dimensional asymmetry. If the vanadate complex is considered to be a stable analogue of the unstable intermediate S1·ϵADP·P_i, which is generated in the Mg^{2+}-dependent ATPase pathway, the anisotropy results suggest a structural difference between S1·ϵADP and S1·ϵADP·P_i. The difference is global and may be interpreted in terms of a dimensionally asymmetric (long correlation time) and dimensionally symmetric structure of S1 in S1·ϵADP and S1·ϵADP·P_i, respectively.

The binding of ϵADP to S1 at room temperature results in $S1_H$·ϵADP predominantly. The ratio of $S1_H$·ϵADP/$S1_L$·ϵADP is 14:1 at 25 °C and 5:1 at 10 °C. Formation of $S1^+$·ϵADP·Vi at the latter temperature is accompanied by a decrease of this ratio to 0.7. In the ternary vanadate complex the low-temperature state $S1_L$·ϵADP predominates. It is currently accepted that the power stroke of the contractile cycle occurs concomitantly with the release of phosphate (Eisenberg & Greene, 1980). The power stroke begins with states such as A·M·ATP and A·M·ADP·P_i and ends with A·M·ADP and A·M (where A is actin and M is myosin). The preferred orientation of the S1 moiety of myosin in A·M·ADP·P_i is usually assumed to be 90° and in A·M·ADP 45°. On the basis of NMR results it has been proposed that there is a direct correspondence between the conformation of S1 in S1·ADP and A·S1·ADP and that in S1·ADP·P_i and A·S1·ADP·P_i (Shriver & Sykes, 1981a). Thus the observed transition $S1_L$·ϵADP → $S1_H$·ϵADP may be related to the power stroke. This relationship is analogous to the conversion M^*_RADP → M^*_TADP previously suggested from NMR results as an energy-transducing transition (Shriver & Sykes, 1981b). The fluorescence data further suggest that the power stroke may be coupled to a global change in the dimensional asymmetry of subfragment 1.

There has been considerable interest in the distance between the active site and either SH_1 or SH_2 of S1. This interest arises from the notion that intersite communication between the active site and the actin-binding sites is an important feature in energy transduction (Hiratsuka, 1987). FRET studies of the proximity between the active site and SH_1 are particularly relevant in view of recent studies demonstrating that a strong actin-binding site of S1 may be a segment of the heavy chain that includes SH_1 (Katoh et al., 1985; Suzuki et al., 1987). The energy transfer described here between bound ϵADP and DDPM is the first reported FRET distance between the adenine-binding site and a probe linked to SH_1. A previous study (Perkins et al., 1984b) used ϵADP trapped at the S1 active site by cross-linking SH_1 and SH_2 with bifunctional chromophoric agents as energy acceptors. The distance [$R(2/3)$] between the trapped ϵADP and the acceptor covalently linked to both thiols was reported to be in the range 23–26 Å. While this distance appears compatible with the present results, it should be noted that it was obtained by phase fluorometry and based on the observation of a single lifetime for both bound and trapped ϵADP in the absence of energy transfer. The discrepancy in the number of lifetimes raises the question as to whether the two sets of FRET results can be directly compared.

Two previous studies (Tao & Lamkin, 1981; Cheung et al., 1985) reported the distance between the active site and SH_1 by using IAEDANS attached to the thiol as the energy donor and the trinitrophenyl moiety of TNP·ADP bound to the nucleotide site as energy acceptor. This distance refers to the separation between the centers of the AEDANS chromophore and the TNP ring, which is attached to the ribose of ADP. There are differences between the ϵADP–SH_1 and the TNP·ADP–SH_1 distances. The sites for the adenine ring and the TNP group are physically different. The bound adenine is quite mobile, whereas the bound TNP group has little motional freedom (Cheung et al., 1985). The latter finding makes the use of $R(2/3)$ to describe the TNP·ADP–SH_1 distance unjustified. The lower limit [R(min)] for the TNP–AEDANS distance is 15 Å and that for the ϵ-adenine–DDPM distance is 21 Å. Because of the size of DDPM, the separation between the center of the adenine ring and the sulfur atom of SH_1 could be considerably smaller than 21 Å. The measured FRET distance is likely an average value of a distribution of distances that arise from protein dynamics. We (Cheung et al., 1987) have recently shown that the FRET distance between SH_1 and SH_2 corresponds to the peak distance of a distribution of distances that was recovered from frequency–domain lifetime data. The existence of a distribution of FRET distances has also been demonstrated with troponin I (Lakowicz et al., 1988). On the basis of these studies we suggest that there may also be a distribution of the ϵADP–SH_1 distances in S1 and the separation between the side chain of Cys 707 and the adenine-binding site fluctuates in time. It is these dynamic fluctuations that may lead to interaction between the nucleotide-binding site and SH_1.

Additional evidence is available to indicate global structural changes in S1 when it is incorporated into the stable ternary complex S1·ϵADP·Vi. The ϵADP–SH_1 distance is shorter in the ternary complex than in the binary complex. It should

be noted that this distance appears unperturbed when rigor acto·S1·ϵADP is formed. The distance between bound ϵADP and bound Co^{2+} is less well defined than the other distance because of uncertainty in metal location and binding stoichiometry. The fact that the steady-state emission of bound ϵADP is quenched by $CoCl_2$ is suggestive, but not proof, of energy transfer between them. In fact the steady-state intensity of free ϵATP and ϵADP is very efficiently quenched by Co^{2+} in the range 10^{-5}–10^{-4} M (Vanderkooi et al., 1979; Miki & Wahl, 1985). However, in the presence of this level of Co^{2+} the lifetime of ethenoadenosine phosphates is not affected (Vanderkooi et al., 1979). This result demonstrates that the observed intensity quenching is static, resulting from dark complexes formed between the phosphates and the metal. The data in Figure 4 reflect static quenching as well as additional quenching, if any, by energy transfer. These two types of quenching can be delineated by lifetime measurements. The average lifetime of S1·ϵADP is reduced in the presence of an excess of $CoCl_2$. This reduction may be taken as evidence for energy transfer because the emission decay of ϵADP is not sensitive to collisional (dynamic) quenching by Co^{2+} and does not respond to static quenching by the cation. The calculated transfer distance indicates a very close proximity between the two sites. In the presence of Vi the intensity quenching is more extensive and shifted to lower concentrations of $CoCl_2$. This additional quenching arises from an increase in energy transfer as reflected by a further reduction in $\langle\tau\rangle$. The increased transfer results from a slow transition of S1·ϵADP·Co·Vi to the stable $S1^+$·ϵADP·Co·Vi. The observed rate constant for this transition is comparable to (1) the rate constant for the transition of S1·ϵADP·Vi to $S1^+$·ϵADP·Vi and (2) the rate previously observed with single chromophores (Aguirre et al., 1986) for the transition of S1·ADP·Vi to the stable $S1^+$·ADP·Vi complex. The comparable rates for the transition of initial vanadate complexes to stable complexes strongly suggest that the same structural transition is being monitored by the different spectroscopic signals.

In summary, we have used the etheno derivative of ADP to probe the adenine-binding site of S1. The results demonstrate a temperature-sensitive two-state equilibrium of the S1·ϵADP complex. The two states differ energetically and structurally. Conversion of $S1^+$·ϵADP·Vi to S1·ϵADP results in increases in (1) the rotational correlation time of the nucleotide bound to S1 and (2) the energy transfer distances from bound nucleotide to SH_1 and to bound Co^{2+}. These structural changes, which occur in S1, may be associated with an energy-transducing transition in contraction.

References

Aguirre, R., Gonsoulin, F., & Cheung, H. C. (1986) *Biochemistry 25*, 6827–6835.

Botts, J., Muhlrad, A., Takashi, R., & Morales, M. F. (1982) *Biochemistry 21*, 6903–6905.

Chaussepied, P., Mornet, D., & Kassab, R. (1986) *Biochemistry 25*, 6426–6432.

Cheung, H. C. (1969) *Biochim. Biophys. Acta 194*, 478–485.

Cheung, H. C., & Liu, B. M. (1984) *J. Muscle Res. Cell Motil. 5*, 65–80.

Cheung, H. C., Gonsoulin, F., & Garland, F. (1983) *J. Biol. Chem. 258*, 5775–5786.

Cheung, H. C., Gonsoulin, F., & Garland, F. (1985) *Biochim. Biophys. Acta 832*, 52–62.

Cheung, H. C., Johnson, M. L., Lakowicz, J. R., Joshi, N., & Gryzcynski, I. (1987) *Biophys. J. 51*, 86a.

Eisenberg, E., & Greene, L. (1980) *Annu. Rev. Physiol. 42*, 293–307.

Flamig, D. P., & Cusanovich, M. A. (1981) *Biochemistry 20*, 6760–6767.

Garland, F., & Cheung, H. C. (1976) *FEBS Lett. 66*, 198–201.

Garland, F., & Cheung, H. C. (1979) *Biochemistry 18*, 5281–5289.

Gold, A. H., & Segal, H. L. (1964) *Biochemistry 3*, 778–782.

Goodno, C. C. (1982) *Methods Enzymol. 85*, 116–123.

Goody, R. S., Hofmann, W., Reedy, M. K., Magid, A., & Goodno, C. (1980) *J. Muscle Res. Cell Motil. 1*, 198–199.

Grinvald, A., & Steinberg, I. Z. (1974) *Anal. Biochem. 59*, 583–598.

Harvey, S. C., & Cheung, H. C. (1976) *Biochem. Biophys. Res. Commun. 73*, 865–868.

Harvey, S. C., Cheung, H. C., & Thames, K. E. (1977) *Arch. Biochem. Biophys. 179*, 391–396.

Highsmith, S., & Murphy, A. J. (1984) *J. Biol. Chem. 259*, 14651–14656.

Hiratsuka, T. (1987) *Biochemistry 26*, 3168–3173.

Katoh, T. S., Imae, S., & Morita, F. (1984) *J. Biochem. (Tokyo) 96*, 1223–1230.

Lakowicz, J. R., Gryczynski, I., Cheung, H. C., Wang, C.-K., & Johnson, M. L. (1988) *Biopolymers 27*, 821–830.

Mendelson, R. A., Mowery, P. C., Botts, J., & Cheung, H. C. (1972) *Biophys. J. 12*, 281a.

Mendelson, R. A., Morales, M. F., & Botts, J. (1973) *Biochemistry 12*, 2250–2255.

Miki, M., & Wahl, Ph. (1985) *Biochim. Biophys. Acta 828*, 188–195.

Morita, F. (1967) *J. Biol. Chem. 242*, 4501–4506.

Morita, F. (1977) *J. Biochem. (Tokyo) 81*, 313–320.

Parker, C. A., & Reese, W. T. (1960) *Analyst (London) 85*, 587–598.

Perkins, W. J., Wells, J. A., & Yount, R. G. (1984a) *Biochemistry 23*, 3994–4002.

Perkins, W. J., Weiel, J., Grammer, J., & Yount, R. G. (1984b) *J. Biol. Chem. 259*, 8786–8793.

Rao, A., Martin, P., Reinhart, A. F., & Cantley, L. C. (1979) *Biochemistry 18*, 4505–4516.

Rosenfeld, S. S., & Taylor, E. W. (1984) *J. Biol. Chem. 259*, 11920–11929.

Scott, T. G., Spencer, R. D., Leonard, N. J., & Weber, F. (1970) *J. Am. Chem. Soc. 92*, 687–695.

Seidel, J., & Gergely, J. (1972) *Cold Spring Harbor Symp. Quant. Biol. 37*, 187–193.

Shriver, J. W., & Sykes, B. D. (1981a) *Biochemistry 20*, 2004–2012.

Shriver, J. W., & Sykes, B. D. (1981b) *Biochemistry 20*, 6357–6362.

Shriver, J. W., & Sykes, B. D. (1982) *Biochemistry 21*, 3022–3028.

Sleep, J. A., & Hutton, R. L. (1980) *Biochemistry 19*, 1276–1283.

Spudich, J. A., & Watts, S. (1971) *J. Biol. Chem. 246*, 4866–4871.

Suzuki, R., Nishi, N., Tokura, S., & Morita, F. (1987) *J. Biol. Chem. 262*, 11410–11412.

Tao, T., & Lamkin, M. (1981) *Biochemistry 20*, 5051–5055.

Trybus, K. M., & Taylor, E. W. (1982) *Biochemistry 21*, 1284–1294.

Vanderkooi, J. M., Weiss, C. J., & Woodrow, G. V., III (1979) *Biophys. J. 25*, 263–276.

Wang, C.-K., & Cheung, H. C. (1986) *J. Mol. Biol. 191*, 509–521.
Wells, J. A., & Yount, R. G. (1982) *Methods Enzymol. 85*, 93–116.
Wells, A. C., & Bagshaw, C. R. (1984) *J. Muscle Res. Cell Motil. 5*, 97–112.
Werber, M. M., Szent-Gyorgyi, A. G., & Fasman, G. D. (1972) *Biochemistry 11*, 2872–2882.

Effect of Nucleotide Structure on Cardiac Myosin Subfragment 1 Transient Kinetics†

Jo H. Hazzard, Deborah H. Tollin, and Michael A. Cusanovich*
Department of Biochemistry, University of Arizona, Tucson, Arizona 85721
Received May 17, 1988; Revised Manuscript Received August 31, 1988

ABSTRACT: Transient kinetic data of the hydrolysis of several nucleotides (TTP, CTP, UTP, GTP) by cardiac myosin subfragment 1 (S1) were analyzed to obtain values for the equilibrium constant for nucleotide binding and rate constants for the S1–nucleotide isomerization and the subsequent nucleotide hydrolysis as well as the magnitudes of the relative fluorescence enhancements of the myosin that occur upon isomerization and hydrolysis. These data are compared with data from a previous study with ATP. Nucleotide binding is found to be relatively insensitive to nucleotide ring structure, being affected most by the group at position C6. Isomerization and hydrolysis are more sensitive to nucleotide structure, being inhibited by the presence of a bulky group at position C2. Kinetic parameters decrease as follows: for binding, GTP > UTP ~ TTP > ATP > CTP; for isomerization, ATP > UTP ~ TTP ~ CTP > GTP; for hydrolysis, ATP > TTP > CTP ~ UTP > GTP. Fluorescence enhancements appear to be most dependent upon the relative values of the individual rate constants.

Muscle myosin catalyzes the hydrolysis of ATP as the primary event in energy transduction during muscle contraction. The conversion of chemical energy to mechanical work takes place in vivo in the highly structured environment of the myofibril in which actin is in close association with myosin. In vitro myosin will catalyze ATP hydrolysis in the absence of other contractile proteins, and this simple system has been quite useful for focusing on the interaction of myosin with nucleotide. The sequence of events by which ATP is hydrolyzed by myosin consists of a minimum of three steps (Bagshaw & Trentham, 1974; Johnson & Taylor, 1978)

$$M_0 + T \underset{}{\overset{K_0}{\rightleftharpoons}} M_0{\cdot}T \underset{k_{21}}{\overset{k_{12}}{\rightleftharpoons}} M_1{\cdot}T \underset{k_{32}}{\overset{k_{23}}{\rightleftharpoons}} M_{12}{\cdot}D{\cdot}P_i \qquad (1)$$

where M_0 denotes myosin, M_1 and M_{12} are myosin intermediates and T, D, and P_i refer to ATP, ADP, and inorganic phosphate, respectively. The myosin intermediates are characterized by an enhanced intrinsic fluorescence that can be used to measure the pre-steady-state reactions by stopped-flow spectroscopy.

The majority of kinetic studies to date have focused on the catalytic subfragment of myosin, subfragment 1 (S1),[1] from skeletal muscle [as reviewed by Taylor (1979) and Eisenberg and Hill (1985)]. Cardiac myosin is of interest in that the protein is present as a mixture of isozymes having functional differences that can be correlated with the contractile performance of the heart (Morkin, 1979; Morkin et al., 1983). The data obtained with myosin from normal cardiac tissue (where one isozyme predominates) are useful, then, not only for comparison with skeletal myosin but also for comparison with cardiac isozymes expressed in diseased or damaged tissue.

The first transient kinetic studies of the cardiac protein showed that the combined rate constant for ATP binding (K_0k_{12}) is an order of magnitude lower than that for skeletal S1 (Marston & Taylor, 1980; Taylor & Weeds, 1976). This was confirmed in subsequent studies with improved cardiac S1 preparations (Flamig & Cusanovich, 1983; Smith & Cusanovich, 1984). Transient kinetic analysis of the cardiac protein has since been extended to include a fluorescent ATP derivative (Smith & White, 1985). The individual kinetic constants K_0, k_{12}, k_{23}, and k_{32} and the fluorescence enhancement for M_1 and M_{12} relative to that for M_0 have also been determined for ATP hydrolysis by cardiac S1 by using computer-modeling techniques (Hazzard & Cusanovich, 1986). With this background data for the cardiac S1 reaction, it is now possible to measure the effects of changes in substrate structure on the rate constants for binding (K_0), isomerization (k_{12}), and hydrolysis (k_{23} and k_{32}). In this manner the structural requirements for effective hydrolysis of the nucleotide substrate may be determined.

The hydrolysis of nucleotides having structures analogous to ATP has been previously investigated for skeletal muscle myosin by a variety of techniques [as reviewed in Werber et al. (1972), Seidel (1975), and Eccleston and Trentham (1977)] and for cardiac myosin steady-state hydrolysis (Balint et al., 1978). The results with skeletal myosin indicate the importance of the amino group at position 6 to a maximal fluorescence enhancement upon hydrolysis (Werber et al., 1972; Bagshaw et al., 1974; Seidel, 1975) and to maximal binding of nucleotide measured as $1/K_m$ (Blum, 1960; Kielley et al., 1956). In this work the binding and hydrolysis of a series

† This research was supported by a grant from the Arizona Disease Control Commission.

[1] Abbreviations: S1, myosin subfragment 1; BTP, 1,3-bis[[tris(hydroxymethyl)methyl]amino]propane; MES, 2-(*N*-morpholino)ethanesulfonic acid.

0006-2960/89/0428-0807$01.50/0